

# Hydrogen-Bond-Directed Self-Assembly of D-(+)-Dibenzoyl Tartaric Acid and 4-Aminopyridine: Optical Nonlinearities and Stoichiometry-Dependent Novel Structural Features

Santanu Bhattacharya,<sup>\*,†</sup> Parthasarathi Dastidar,<sup>†</sup> and T. N. Guru Row<sup>†,‡</sup>

Department of Organic Chemistry and Solid State and Structural Chemistry Unit, Indian Institute of Science, Bangalore 560 012, India

Received November 18, 1993. Revised Manuscript Received February 8, 1994<sup>⊙</sup>

Attempts to prepare hydrogen-bond-directed nonlinear optical materials from a 1:1 molar mixture of D-(+)-dibenzoyltartaric acid (DBT, I) and 4-aminopyridine (4-AP, II) resulted in two salts of different stoichiometry. One of them crystallizes in an unusual 1.5:1 (acid:base) monohydrate salt form III while the other one crystallizes as 1:1 (acid:base) salt IV. Crystal structures of both of the salts were determined from single-crystal X-ray diffraction data. The salt III crystallizes in a monoclinic space group  $C2$  with  $a = 30.339(1)$ ,  $b = 7.881(2)$ ,  $c = 14.355(1)$  Å,  $\beta = 97.48(1)^\circ$ ,  $V = 3403.1(9)$  Å<sup>3</sup>,  $Z = 4$ ,  $R = 0.058$ ,  $R_w = 0.058$ . The salt IV also crystallizes in a monoclinic space group  $P2_1$  with  $a = 7.500(1)$ ,  $b = 14.968(2)$ ,  $c = 10.370(1)$  Å,  $\beta = 102.67(1)^\circ$ ,  $V = 1135.9(2)$  Å<sup>3</sup>,  $Z = 2$ ,  $R = 0.043$ ,  $R_w = 0.043$ . Interestingly, two DBT molecules with distinctly different conformation are present in the same crystal lattice of salt III. Extensive hydrogen-bonding interactions are found in both of the salts, and both of them show SHG intensity 1.4–1.6 times that of urea.

## Introduction

Nonlinear optical (NLO) materials<sup>1</sup> are of current research interest in material science for their applications in second and third harmonic generation,<sup>2</sup> optical bistability,<sup>3</sup> laser remote sensing, optical disk data storage, laser-driven fusion, and medical and spectroscopic laser.<sup>4</sup> Even though commercially available NLO crystalline materials, e.g., potassium niobate,<sup>5</sup> lithium niobate,<sup>6</sup> potassium dihydrogen phosphate,<sup>7</sup> and  $\beta$ -barium borate,<sup>8</sup> are usually of inorganic origin, organic NLO materials are of appreciable current interest.<sup>9</sup> This is because they are

generally more amenable to structural variations than their inorganic counterparts. Additionally, organic molecules possess larger second-order molecular hyperpolarizability ( $\beta$ ), more favorable physical (large optical damage threshold and large birefringence) properties and are more versatile in synthetic manipulations. Until very recently, synthetic efforts on organic NLO materials have been mainly concentrated on tuning molecular structure (e.g., by increasing the conjugation chain length of a donor-acceptor-based chromophore or by alteration of the strength of donor and acceptor of a chromophore etc.) so as to achieve larger  $\beta$  values and hence larger NLO response.<sup>10,11</sup> But large  $\beta$  values do not necessarily guarantee an excellent NLO response, viz., second harmonic generation (SHG) due to frequent occurrence in the form of centrosymmetric crystals or unfavorable packing of the molecules in the crystal.<sup>12</sup> Our efforts to design, synthesize, and characterize "push-pull" ethylenes and butadienes as NLO organic materials did not elicit significant NLO response due to either the centrosymmetric nature of the crystals or mutual cancellation of molecular dipoles during crystal packing.<sup>13-17</sup> We thought that further efforts toward the design and synthesis of similar conjugated systems would be complicated because attempts to enhance the nonlinearity in terms of  $\beta$  value

<sup>†</sup> Department of Organic Chemistry.

<sup>‡</sup> Solid State and Structural Chemistry Unit.

<sup>⊙</sup> Abstract published in *Advance ACS Abstracts*, March 15, 1994.

(1) Prasad, P. N.; Williams, D. J. *Introduction to Nonlinear Optical Effects in Molecules and Polymers*; Wiley: New York, 1990.

(2) Williams, D. J. *Electronic and Photonic Applications of Polymers*; Bowden, M. J., Turner, S. R., Eds.; American Chemical Society: Washington, DC, 1988; p 218.

(3) (a) Hunsperger, R. G. *Integrated Optics: Theory and Technology*, 2nd ed.; Springer-Verlag: New York, 1984; p 127. (b) Ulrich, D. R. *Mol. Cryst. Liq. Cryst.* 1990, 189, 3.

(4) Bourhill, G.; Mansour, K.; Perry, K. J.; Khundkar, L.; Sleva, E. T.; Kern, R.; Perry, J. W.; Williams, I. D.; Kurtz, S. K. *Chem. Mater.* 1993, 5, 802.

(5) Biaggio, L.; Kerkoc, P.; Wu, L. S.; Gunter, P. J. *Opt. Soc. Am. B.* 1992, 9, 507.

(6) Miller, R. C.; Boyd, G. D.; Savage, A. *Appl. Phys. Lett.* 1965, 6, 77.

(7) Marker, P. D.; Terhune, R. W.; Nisenoff, M.; Savage, C. M. *Phys. Rev. Lett.* 1962, 8, 21.

(8) (a) Chen, C. *Materials for Nonlinear Optics*; Marder, S. R., Sohn, J. E., Stucky, G. D., Eds.; ACS Symposium Series 455; American Chemical Society: Washington, DC, 1991; p 360. (b) Eimerl, D.; Davis, L.; Velsko, S.; Graham, E. k.; Zalkin, A. J. *Appl. Phys.* 1987, 62, 1968.

(9) (a) Grubbs, R. B.; Marder, S. R.; Perry, J. W. *Chem. Mater.* 1991, 3, 3. (b) Bella, S. D.; Fragale, I. L.; Ratner, M. A.; Marks, T. J. *J. Am. Chem. Soc.* 1993, 115, 682. (c) Chaput, F.; Riehl, D.; Levy, Y.; Boilot, Jean-Pierre. *Chem. Mater.* 1993, 5, 589. (d) Marturunkakul, S.; Chen, J. L.; Li, L.; Jeng, R. J.; Kumar, J.; Tripathy, S. K. *Chem. Mater.* 1993, 5, 592. (e) Agrawal, A. K.; Jenekhe, S. A. *Chem. Mater.* 1993, 5, 633. (f) Francis, C. V.; White, K. M.; Boyd, G. T.; Moshrefazadeh, R. S.; Mohapatra, S. K.; Radcliffe, M. D.; Trend, J. E.; Williams, R. C. *Chem. Mater.* 1993, 5, 506. (g) Mitchell, M. A.; Tomida, M.; Padias, A. B.; Hall, Jr., H. K.; Lackritz, H. S.; Robello, D. R.; Willand, C. S.; Williams, D. J. *Chem. Mater.* 1993, 5, 1044.

(10) *Nonlinear Optical Properties of Organic Molecules and Crystals*; Chemla, D. S., Zyss, J., Eds.; Academic Press: New York, 1987; Vols. 1, 2.

(11) *Materials for Nonlinear Optics*; Marder, S. R., Sohn, J. E., Stucky, G. D., Eds.; ACS Symposium Series 455; American Chemical Society: Washington, DC, 1991.

(12) Zyss, J.; Oudar, J. L. *Phys. Rev.* 1982, A26, 2028.

(13) Kanagapushpam, D.; Venkatesan, K. *Acta Crystallogr., Sect. C, Cryst. Struct. Commun.* 1987, 43, 1597.

(14) Kanagapushpam, D.; Padmanabhan, K.; Venkatesan, K. *Acta Crystallogr., Sect. C, Cryst. Struct. Commun.* 1987, 43, 1717.

(15) Kanagapushpam, D.; Venkatesan, K.; Cameron, T. S. *Acta Crystallogr., Sect. C, Cryst. Struct. Commun.* 1988, 44, 337.

(16) Dastidar, P.; Guru Row, T. N.; Venkatesan, K. *J. Mater. Chem.* 1991, 1, 1057.

(17) Dastidar, P.; Guru Row, T. N.; Venkatesan, K. *Acta Crystallogr., Sect. B, Struct. Sci.* 1993, B49, 900.

Table 1. Physical Data of Salts III and IV

Salt III	
color	colorless
mp (°C)	138 (dec)
optical rotation	$[\alpha]_{25}^{25} = +166.6^\circ$ ( $c = 0.06$ , MeOH)
IR (KBr pellet)	3395 (hydrate), 3190 (protonated amine), 1702 (–COOH), strong stretch at 1591 and weak absorption at 1401 $\text{cm}^{-1}$ (–COO–)
C, H, N analysis (obsd, theor) <sup>a</sup>	C 58.70%, 59.16%; H 4.37%, 4.47%; N 4.24%, 4.31%
Salt IV	
color	colorless
mp (°C)	142 (dec)
optical rotation	$[\alpha]_{25}^{25} = +250.0^\circ$ ( $c = 0.036$ , MeOH)
IR (KBr pellet)	3290, 3148 (protonated amine), 1715 (hydrogen-bonded –COOH dimer), strong stretch at 1583 and weak absorption at 1407 $\text{cm}^{-1}$ (–COO–)
C, H, N analysis (obsd, theor) <sup>b</sup>	C 61.08%, 61.00%; H 4.55%, 4.45%; N 6.25%, 6.18%

<sup>a</sup> Confirmed after solving the X-ray crystal structure. <sup>b</sup> Stoichiometry 1:1.

would require large dipole moment difference between ground state and excited state which in turn would necessitate strong  $\pi$ -electron conjugation between donor and acceptor across the chromophoric moiety. This often leads to a decrease in the ultraviolet/visible transparency of the materials, the so called nonlinearity–transparency tradeoff.<sup>18</sup>

An alternative and presumably more general strategy would be to achieve an orientation of the net dipoles of a set of ions, molecules, or molecular assemblies in a crystal to a particular direction. A primary advantage of this strategy is that complex structures with specific structural features are formed through inter- and intramolecular noncovalent forces and not by tedious bond-by-bond syntheses. This may also assist in maximum NLO effect which is obviously more important than having a large  $\beta$  value in the molecular level. Crystal engineering<sup>19,20</sup> is a powerful technique that allows one to elucidate relationships between molecular structure and specific solid-state properties in a predictable manner. On the basis of their inter- and intramolecular force fields for a variety of organic materials, crystal structures have indeed been calculated.<sup>21</sup> Since there exists a satisfactory agreement with experimentally observed unit-cell parameters, rational conclusions can be drawn using this approach.<sup>21</sup> Therefore, analysis and study of such relationship should provide useful insights to addressing this problem. In this context, it may also be pointed out that the major drawback associated with organic materials in using them in commercial NLO devices is the lack of quality and/or the size of the bulk crystals. The organic crystals are often soft and cannot be cut or polished using standard optical techniques. Therefore, it would be useful to prepare systems that involve multidirectional hydrogen bonding so as to produce good-quality crystals. Additionally, the potential utility of such materials is mainly in their hardness to mechanical damage and thermal and optical stability relative to urea. Such physical properties should make their handling and use more satisfactory. L-Tartaric

Table 2. Crystal Data and Intensity Collection for Salts III and IV

	[DBT] <sub>1.6</sub> [4-AP]H <sub>2</sub> O (III)	[DBT][4-AP] (IV)
mol formula	C <sub>32</sub> H <sub>27</sub> O <sub>12</sub> N <sub>2</sub> ·H <sub>2</sub> O <sup>a</sup>	C <sub>23</sub> H <sub>20</sub> O <sub>8</sub> N <sub>2</sub>
mol wt	649.5	452.4
cryst syst	monoclinic	monoclinic
space group	C2	P2 <sub>1</sub>
a/Å	30.339(1)	7.500(1)
b/Å	7.881(2)	14.968(2)
c/Å	14.355(1)	10.370(1)
$\beta/^\circ$	97.48(1)	102.67(1)
V/Å <sup>3</sup>	3403.1(9)	1135.9(2)
Z	4	2
D <sub>c</sub> /g cm <sup>-3</sup>	1.267	1.322
D <sub>m</sub> <sup>b</sup> /g cm <sup>-3</sup>	1.272	1.321
cryst size/mm	0.25 × 0.12 × 0.12	0.45 × 0.35 × 0.40
radiation used	Mo K $\alpha$	Mo K $\alpha$
temp/°C	22	22
wavelength/Å	0.7107	0.7107
$\mu/\text{cm}^{-1}$	0.932	0.948
temp/K	295	295
F(000)	1356	472
scan mode	$\omega/2\theta$	$\omega/2\theta$
no. of reflns for measuring lattice parameters <sup>c</sup>	25, 6 ≤ $\theta$ ≤ 15	25, 7 ≤ $\theta$ ≤ 16
$\theta$ range for data collection <sup>c</sup>	0 ≤ $\theta$ ≤ 23.5	0 ≤ $\theta$ ≤ 25.1
range of h	0 → 34	0 → 8
range of k	0 → 8	0 → 16
range of l	-16 → 16	-11 → 11
no. of reflns measd	2791	2086
no. of unique reflns	2728	1868
no. of significant reflns [ $F_o$ ] ≥ 3 $\sigma$ ( $F_o$ )	1467	1768
final R (R <sub>w</sub> )	0.058 (0.058)	0.043 (0.043)
weighting	1.0	1.0
no. of params	424	298
S, goodness of fit	2.16	0.59
$\Delta\rho_{\text{min}}$ ; $\Delta\rho_{\text{max}}$	+0.07; -0.08	+0.09; -0.12

<sup>a</sup> Derived after structure solution. <sup>b</sup> Benzene–bromoform mixture. <sup>c</sup>  $\theta$  in degrees.

acid is a chiral dihydroxydicarboxylic acid. Therefore, it should be capable of initiating multidirectional hydrogen bonding.<sup>22</sup> On the basis of this property, a new class of NLO-active materials has been prepared through salt formation of various organic bases with it.<sup>23,24</sup> Systematic investigations reveal the crucial relationship between packing of the molecules in the crystal and the quantum of SHG intensity in these salts.<sup>24</sup> The propensity of the individual components to form several well-directed hydrogen bonds in these binary salts resulting in NLO materials indicates that a newer supramolecular network could be generated by suitable modification of the individual partners. Modifications such as transformation of hydroxyl groups in L-tartaric acid into O-benzoyl ester could convert them into hydrogen bond acceptors. In addition, this offers a potential for interactions through interaromatic stacks. Consequently in this study, we have employed D-(+)-dibenzoyltartaric acid (DBT, I) as one of the partners. DBT being a chiral molecule ensures the noncentrosymmetry of the crystal. When we attempted to prepare such salts, we obtained two salts of different stoichiometry from I and 4-aminopyridine (4-AP, II). The single-crystal X-ray analysis of both of the salts were performed in order to understand the effect of structural

(18) Ledoux, I.; Zyss, J.; Jutand, A.; Amatore, C. *Chem. Phys.* 1991, 150, 117.

(19) Desiraju, G. R. *Crystal Engineering. The Design of Organic Solids*; Elsevier: Amsterdam, 1989.

(20) Lehn, J.-M. *Angew. Chem., Int. Ed. Engl.* 1990, 29, 1304.

(21) (a) Warshel, A.; Lifson, S. *J. Chem. Phys.* 1970, 52. (b) Gavezzotti, A. *J. Am. Chem. Soc.* 1991, 113, 4622.

(22) *The Hydrogen Bond*; Schuster, D., Zundel, G., Zandorfy, C., Eds.; North-Holland: Amsterdam, 1976; Vols. I–III.

(23) (a) Aakeroy, C. B.; Hitchcock, P. B.; Seddon, K. R. *J. Chem. Soc., Chem. Commun.* 1992, 553. (b) Zyss, J.; Masse, R.; Bagieu-Beucher, M.; Levy, J.-P. *Adv. Mater.* 1993, 5, 120 and references therein.

(24) Dastidar, P.; Guru Row, T. N.; Prasad, B. R.; Subramanian, C. K.; Bhattacharya, S. *J. Chem. Soc., Perkin Trans. 2* 1993, 2419.

**Table 3. Atomic and Isotropic Thermal Parameters ( $\times 10^4$ ) for Salt III**

atom	X/A	Y/B	Z/C	$U_{eq}$ ( $\text{\AA}^2$ ) <sup>a</sup>
C1	0.1879(5)	0.2557(15)	-0.0126(8)	824(35)
C2	0.2288(5)	0.2933(19)	0.0326(10)	1047(40)
C3	0.2649(5)	0.3095(24)	-0.0185(12)	1417(41)
C4	0.2586(7)	0.2807(29)	-0.1105(14)	1774(44)
C5	0.2201(8)	0.2390(28)	-0.1563(10)	1832(44)
C6	0.1822(5)	0.2225(21)	-0.1087(8)	1193(40)
C7	0.1493(4)	0.2314(14)	0.0367(8)	714(34)
C8	0.1226(3)	0.2370(12)	0.1846(7)	506(30)
C9	0.1260(3)	0.3748(12)	0.2609(6)	482(32)
C10	0.1671(4)	0.3997(13)	0.4121(7)	671(37)
C11	0.2107(4)	0.4004(14)	0.4672(7)	653(32)
C12	0.2476(5)	0.3783(24)	0.4281(9)	1223(43)
C13	0.2883(5)	0.3810(26)	0.4834(13)	1498(44)
C14	0.2915(6)	0.4043(19)	0.5782(12)	1185(41)
C15	0.2539(6)	0.4251(27)	0.6136(10)	1418(43)
C16	0.2130(5)	0.4250(25)	0.5604(9)	1260(41)
C17	0.1249(4)	0.0566(13)	0.2254(7)	526(32)
C18	0.1241(4)	0.5525(13)	0.2125(7)	532(31)
OS	0.0694(2)	0.7207(11)	0.3666(5)	821(26)
O1	0.1124(3)	0.1953(11)	0.0009(5)	884(29)
O2	0.1582(2)	0.2645(8)	0.1299(4)	542(20)
O3	0.1331(3)	0.4491(12)	0.4397(5)	911(30)
O4	0.1672(2)	0.3553(8)	0.3219(4)	532(22)
O5	0.1467(2)	-0.0484(8)	0.1853(4)	594(24)
O6	0.1031(3)	0.0279(9)	0.2907(5)	758(26)
O7	0.0965(3)	0.5766(10)	0.1452(5)	773(28)
O8	0.1534(2)	0.6565(9)	0.2515(5)	652(25)
C19	-0.0911(4)	0.5828(19)	0.3402(9)	881(35)
C20	-0.1231(5)	0.5906(22)	0.2674(11)	1319(41)
C21	-0.1466(7)	0.7350(33)	0.2426(11)	1811(44)
C22	-0.1366(5)	0.8696(28)	0.2983(12)	1721(41)
C23	-0.1031(5)	0.8767(19)	0.3741(11)	1297(41)
C24	-0.0801(4)	0.7218(19)	0.3981(8)	924(39)
C25	-0.0684(4)	0.4111(18)	0.3553(9)	879(34)
C26	-0.0098(2)	0.2712(11)	0.4494(6)	456(26)
C27	0.0239(3)	0.2584(14)	0.3834(7)	574(31)
O9	-0.0769(3)	0.2881(12)	0.3130(7)	1198(33)
O10	-0.0362(2)	0.4175(9)	0.4319(4)	603(22)
O11	0.0269(2)	0.3551(9)	0.3196(5)	723(24)
O12	0.0499(2)	0.1272(9)	0.4012(5)	841(26)
C28	-0.0571(4)	0.7910(14)	0.0689(7)	784(34)
C29	-0.0424(4)	0.9036(14)	0.1423(8)	967(33)
C30	-0.0128(4)	0.8464(18)	0.2149(8)	943(36)
C31	-0.0132(4)	0.5811(15)	0.1527(8)	873(34)
C32	-0.0419(4)	0.6215(14)	0.0784(8)	777(32)
N1	0.0009(3)	0.6890(14)	0.2196(6)	879(32)
N2	-0.0851(4)	0.8371(12)	-0.0049(6)	1133(31)

$$^a U_{eq} = \frac{1}{3} \sum_i \sum_j U_{ij} a_i^* a_j^* \hat{a}_i \hat{a}_j$$

modification on the acid counterpart. In this paper, we present the detailed crystal structures of both of the salts and SHG activities of individual crystalline salts which were estimated by using standard powder technique (see below).

### Experimental Section

IR spectra of the salts in KBr pellet were recorded on a Perkin-Elmer Model 781 spectrometer. Optical rotation measurements were obtained from a JASCO, Model DIP-370. Acid-base salt was prepared by dissolving equimolar amounts of I and II in wet methanol and then allowing the solvent to evaporate slowly at room temperature. Crystals, then formed, were filtered from the mother liquor and recrystallized from 1:1 aqueous methanol, filtered, and dried. Examination under the microscope indicated that there were two different kinds of crystals with distinctly different morphology, one was needle shaped (salt III) and the other one was prismatic (salt IV). They were separated manually under the microscope. Density measurements and X-ray powder diffraction patterns confirmed that they were indeed different from each other. They were then subjected to several physico-chemical characterization, e.g., melting point measurements, solid-state IR, optical rotation determinations, and C, H, N analyses. The results are summarized in Table 1.

**Table 4. Atomic and Isotropic Thermal Parameters ( $\times 10^4$ ) for Salt IV**

atom	X/A	Y/B	Z/C	$U_{eq}$ ( $\text{\AA}^2$ ) <sup>a</sup>
C1	0.1749(6)	0.3974(4)	0.4397(4)	410(10)
C2	0.1928(7)	0.4691(4)	0.3577(5)	491(11)
C3	0.1975(8)	0.5559(4)	0.4075(6)	619(11)
C4	0.1790(8)	0.5704(5)	0.5368(6)	704(11)
C5	0.1607(8)	0.4990(5)	0.6175(5)	703(11)
C6	0.1622(7)	0.4120(4)	0.5710(5)	548(11)
C7	0.1672(5)	0.3037(4)	0.3909(4)	395(10)
C8	0.1319(5)	0.2134(3)	0.2008(4)	333(9)
C9	0.1914(5)	0.2194(3)	0.0707(4)	353(10)
C10	0.0094(6)	0.2625(4)	-0.1373(5)	465(11)
C11	-0.1243(6)	0.3286(4)	-0.2063(5)	515(10)
C12	-0.1781(7)	0.4024(5)	-0.1408(6)	713(12)
C13	-0.3047(8)	0.4639(5)	-0.2150(8)	947(12)
C14	-0.3697(8)	0.4464(6)	-0.3506(8)	1068(12)
C15	-0.3180(9)	0.3741(6)	-0.4136(7)	940(12)
C16	-0.1944(8)	0.3149(5)	-0.3419(6)	711(11)
C17	-0.0713(6)	0.1871(4)	0.1761(4)	395(10)
C18	0.3915(6)	0.2475(4)	0.0877(4)	391(9)
O1	0.1616(5)	0.2388(3)	0.4587(3)	566(9)
O2	0.1649(4)	0.3001(2)	0.2618(3)	344(8)
O3	0.0571(6)	0.1975(3)	-0.1877(4)	780(9)
O4	0.0732(4)	0.2835(2)	-0.0092(3)	397(9)
O5	-0.1762(4)	0.2389(3)	0.2186(3)	529(9)
O6	-0.1100(5)	0.1166(3)	0.1164(4)	576(9)
O7	0.4972(4)	0.1973(3)	0.1726(3)	547(9)
O8	0.4372(4)	0.3071(3)	0.0230(4)	523(9)
C19	0.5234(6)	0.0333(3)	0.8757(4)	474(10)
C20	0.5426(7)	0.1265(3)	0.8495(5)	523(10)
C21	0.4327(7)	0.1628(4)	0.7408(5)	629(10)
C22	0.2839(7)	0.0271(4)	0.6805(5)	639(10)
C23	0.3850(6)	-0.0146(4)	0.7866(5)	553(11)
N1	0.3082(6)	0.1138(3)	0.6575(4)	665(10)
N2	0.6309(6)	-0.0044(3)	0.9789(4)	585(11)

$$^a U_{eq} = \frac{1}{3} \sum_i \sum_j U_{ij} a_i^* a_j^* \hat{a}_i \hat{a}_j$$

SHG were measured by using standard powder technique.<sup>25</sup> The samples used were microcrystalline powders, obtained respectively by grinding of III and IV. Individual samples were held between two glass cover slides, with the sample thickness (1.0 mm) kept constant in all experiments. The gross distribution of particle sizes ranged from about 5 to 50  $\mu\text{m}$ . A pulsed Q-switched Nd:YAG laser (Quanta Ray DCR-2A) with a pulse duration of 10 ns at 1.06  $\mu\text{m}$  was used to generate a second harmonic generation signal from the samples. The forward scattered SHG signals were collected using a collection optics and passed through a filter which transmits only the 532-nm radiation. The intensities of the incident laser beam and SHG radiation were measured using an energy ratio meter (LPC RJ-7620) equipped with pyroelectric (LPC RJP-735) and silicon (LPC RJP-765) detector. Measured SHG intensities of samples were normalized with respect to that of urea.

Data were collected (for both the salts) on an Enraf Nonius CAD-4 diffractometer using MoK $\alpha$  ( $\lambda = 0.7107 \text{\AA}$ ) radiation in  $\omega/2\theta$  scan mode. A prescan speed of 5.5°/min was employed, and the final scan was done with a scan speed calculated to satisfy the condition  $\sigma(I)/I \leq 0.03$  for all reflections. The stability and orientation in both of the cases were monitored by measuring three standard reflections (714, 14 04, 531, for III; 132, 143, 153  $\rightarrow$  intensity and 195, 282, 063  $\rightarrow$  orientation for IV) after every 3600 s of exposure time; the orientation was checked after every 400 reflections, and no significant fluctuation in their intensities was observed. The data were corrected for Lorentz and polarization effects, but not for extinction and absorption effects. Details of the data collection, reduction, and refinement are summarized in Table 2.

The structure solution of III was not straightforward. The compound could crystallize either in C2 or Cm (C2/m is ruled out because the chirality in the system ensures noncentrosymmetry). A direct method run using SHELXS86<sup>26</sup> did not give any meaningful structure in both Cm and C2 space groups. However, only a small fragment with meaningful contacts and angles could

**Table 5. Anisotropic Thermal Parameters ( $\times 10^4$ ) for Salt III**

atom	U11	U22	U33	U23	U13	U12
C1	1270(66)	499(56)	762(57)	3(54)	353(56)	249(59)
C2	1249(68)	957(68)	1024(64)	70(62)	488(63)	105(67)
C3	1320(71)	1553(78)	1514(73)	247(72)	694(68)	248(72)
C4	1985(77)	1883(80)	1688(76)	353(76)	1118(71)	484(78)
C5	2804(80)	2007(80)	927(64)	214(72)	1155(67)	754(78)
C6	1740(73)	1199(71)	704(58)	20(63)	398(61)	561(68)
C7	998(63)	361(51)	830(60)	106(52)	294(56)	196(54)
C8	639(53)	251(45)	641(51)	140(43)	130(46)	58(45)
C9	671(54)	234(44)	547(49)	91(43)	97(45)	92(45)
C10	1253(67)	337(50)	476(51)	60(45)	314(52)	4(55)
C11	944(62)	480(54)	548(51)	68(48)	144(51)	82(54)
C12	870(64)	1781(77)	1027(65)	442(69)	159(61)	328(69)
C13	847(66)	1875(79)	1730(75)	756(75)	5(69)	159(71)
C14	1364(72)	679(62)	1567(74)	377(66)	395(70)	298(66)
C15	1334(73)	1951(79)	969(67)	495(72)	148(66)	97(76)
C16	1210(70)	1800(77)	748(62)	270(69)	50(60)	197(73)
C17	624(55)	342(50)	636(54)	58(48)	177(47)	52(48)
C18	837(60)	319(49)	503(50)	106(47)	329(47)	17(51)
OS	921(46)	650(44)	877(44)	66(42)	66(38)	98(43)
O1	1177(53)	682(48)	800(46)	84(41)	150(42)	288(46)
O2	880(42)	303(34)	491(36)	23(31)	270(32)	106(34)
O3	1185(53)	1006(55)	571(40)	14(43)	225(40)	264(50)
O4	726(41)	199(31)	679(39)	16(32)	126(33)	15(31)
O5	908(46)	292(35)	642(38)	83(32)	327(35)	53(37)
O6	1234(53)	257(34)	920(44)	69(35)	662(42)	43(39)
O7	1069(50)	470(42)	772(45)	104(39)	89(41)	46(42)
O8	953(45)	264(34)	755(41)	8(33)	167(36)	222(37)
C19	488(52)	1241(66)	902(58)	599(57)	42(48)	181(55)
C20	994(65)	1504(72)	1432(69)	621(66)	57(63)	61(66)
C21	1810(76)	2448(79)	1203(69)	490(75)	298(68)	149(77)
C22	644(57)	2779(77)	1762(71)	1261(70)	236(61)	811(66)
C23	1051(65)	1080(66)	1801(72)	427(67)	340(64)	358(63)
C24	653(56)	1097(65)	1038(60)	265(62)	169(51)	112(58)
C25	484(52)	956(63)	1171(63)	274(61)	14(53)	96(57)
C26	264(40)	395(45)	710(46)	52(41)	62(37)	88(40)
C27	486(47)	530(51)	719(51)	55(49)	129(43)	27(47)
O9	1430(59)	794(50)	1444(58)	182(49)	466(50)	341(52)
O10	442(33)	650(40)	713(37)	17(36)	56(29)	7(35)
O11	824(43)	560(39)	830(40)	259(38)	275(35)	110(36)
O12	1027(46)	611(40)	1000(46)	197(38)	567(38)	202(41)
C28	1150(60)	542(51)	668(51)	20(47)	149(50)	67(54)
C29	1496(66)	519(52)	886(57)	69(53)	157(57)	234(57)
C30	1194(63)	977(62)	629(52)	184(55)	14(52)	102(60)
C31	1204(63)	706(57)	765(54)	69(54)	342(53)	213(56)
C32	954(58)	559(53)	803(55)	41(48)	62(50)	165(52)
N1	906(52)	962(57)	805(50)	232(50)	251(44)	257(50)
N2	1965(65)	654(50)	851(51)	97(47)	449(53)	301(54)

be extracted from the E-map in C2. Subsequent phase expansions using this fragment as a starting model eventually gave all non-hydrogen atoms which showed that it was a DBT:4-AP monohydrate salt with an unusual 1.5:1 stoichiometry. On the other hand, all the non-hydrogen atoms of IV appeared on the E-map by a direct method run. In both the cases, the direct method program SHELXS86<sup>26</sup> was used for calculations. All the non-hydrogen atoms in both the cases were refined anisotropically using SHELX76.<sup>27</sup> In III, hydrogen attached to solvent oxygen, OS, pyridine ring nitrogen, N1, and one of the COOH oxygen, O8, were located on a difference Fourier map and their positional and thermal parameters were refined for a few cycles. The other hydrogens are at their calculated positions and refined for a few cycles. None of the hydrogen parameters were refined in the final cycles of refinement, but their contributions to structure factor calculations were considered. In IV, hydrogen attached to one of the COOH oxygen, O7, was located on a difference Fourier map and its positional and thermal parameters were refined for a few cycles and kept fixed for the rest of the cycles of refinements. The other hydrogens are at their calculated positions, and none of them were refined but their contributions

(26) Sheldrick, G. M. *SHELXS86. Program for the solution of crystal structures*; University of Göttingen: Germany, 1986.

(27) Sheldrick, G. M. *SHELX76. Program for crystal structure determinations*; University of Cambridge: England, 1976.

**Table 6. Anisotropic Thermal Parameters ( $\times 10^4$ ) for Salt IV**

atom	U11	U22	U33	U23	U13	U12
C1	361(16)	469(17)	388(16)	19(15)	57(15)	3(15)
C2	540(17)	478(17)	468(17)	45(16)	140(16)	40(17)
C3	732(19)	484(18)	636(18)	34(17)	139(17)	6(17)
C4	688(18)	671(18)	750(19)	305(18)	150(18)	78(18)
C5	791(19)	837(19)	510(17)	241(17)	204(17)	54(18)
C6	595(18)	668(19)	411(16)	41(17)	176(16)	2(17)
C7	289(15)	508(17)	380(16)	18(16)	53(14)	15(16)
C8	254(15)	354(16)	385(15)	12(14)	59(13)	26(14)
C9	288(15)	352(16)	409(15)	26(15)	56(14)	28(14)
C10	348(16)	624(18)	412(16)	57(16)	59(15)	38(16)
C11	370(16)	571(18)	562(17)	186(17)	12(15)	61(16)
C12	520(18)	735(19)	853(19)	190(18)	83(17)	153(18)
C13	622(18)	716(19)	1525(20)	318(20)	282(19)	172(18)
C14	465(18)	1322(20)	1406(20)	888(19)	179(19)	153(19)
C15	824(19)	1067(20)	944(20)	493(19)	225(19)	228(19)
C16	695(18)	789(19)	617(18)	262(18)	77(17)	219(18)
C17	271(15)	472(17)	415(16)	109(16)	18(14)	54(15)
C18	344(15)	383(16)	481(16)	102(15)	165(14)	19(15)
O1	776(16)	476(15)	424(14)	114(13)	81(13)	11(14)
O2	333(12)	360(13)	341(12)	28(11)	78(10)	55(12)
O3	921(17)	856(18)	500(15)	242(15)	21(15)	276(17)
O4	380(13)	408(14)	379(13)	0(12)	28(11)	75(12)
O5	249(12)	634(16)	708(15)	32(14)	111(12)	12(13)
O6	434(14)	554(15)	716(16)	92(14)	74(13)	190(13)
O7	250(13)	680(16)	697(15)	223(15)	74(12)	12(13)
O8	476(14)	395(14)	744(15)	43(14)	234(13)	38(13)
C19	535(16)	411(16)	490(16)	20(15)	118(15)	11(15)
C20	605(17)	420(16)	578(16)	2(15)	205(15)	19(16)
C21	705(17)	508(17)	744(17)	181(16)	308(16)	167(16)
C22	513(16)	773(18)	578(17)	93(17)	4(16)	89(17)
C23	530(17)	519(17)	557(16)	63(16)	6(15)	3(16)
N1	645(16)	832(18)	502(15)	157(15)	93(14)	249(16)
N2	746(17)	428(15)	585(16)	55(14)	157(15)	137(15)

**Table 7. Selected Bond Distances (angstroms) and Angles (degrees) of 4-AP Moiety in Salt III and IV and Its Protonated Analogues**

	corresponding distances and angles in		
	salt III	salt IV	free 4-AP hemiperchlorate
N(2)-C(28) =	1.319(13)	1.317(5)	1.363(3)
C(30)-N(1)-C(31) =	120.4(10)	121.1(4)	115.1(2)
			120.2(3)

**Table 8. Backbone Torsion Angles (degrees) of DBT-G and DBT-C2 in Salt III and DBT in Salt IV**

torsion angles/deg	DBT-G	DBT-C2	DBT
C(17)-C(8)-C(9)-C(18)	179.1(8)	-171.5(1)	178.6(3)
O(2)-C(8)-C(9)-O(4)	-63.1(8)	-60.8(1)	-63.9(3)

to structure factor calculations were considered in the final cycles of refinement.

## Results and Discussion

Final atomic coordinates and equivalent isotropic thermal parameters of non-hydrogens of III are given in Table 3 and those for IV are in Table 4. Anisotropic thermal parameters are given in Tables 5 and 6.

**Crystal Structure of Salt III.** An ORTEPII<sup>28</sup> view of the asymmetric unit with atom numbering scheme and the stereo packing diagram of the salt III is shown in the Figure 1. A general feature of the crystal structure of diacyltartaric acids shows a conformation in which the -COOH groups are anti and the O-acyl groups are gauche

(28) Johnson, C. K. *ORTEPII. Report ORNL-5138*; Oak Ridge National Laboratory: Oak Ridge, TN, 1976.

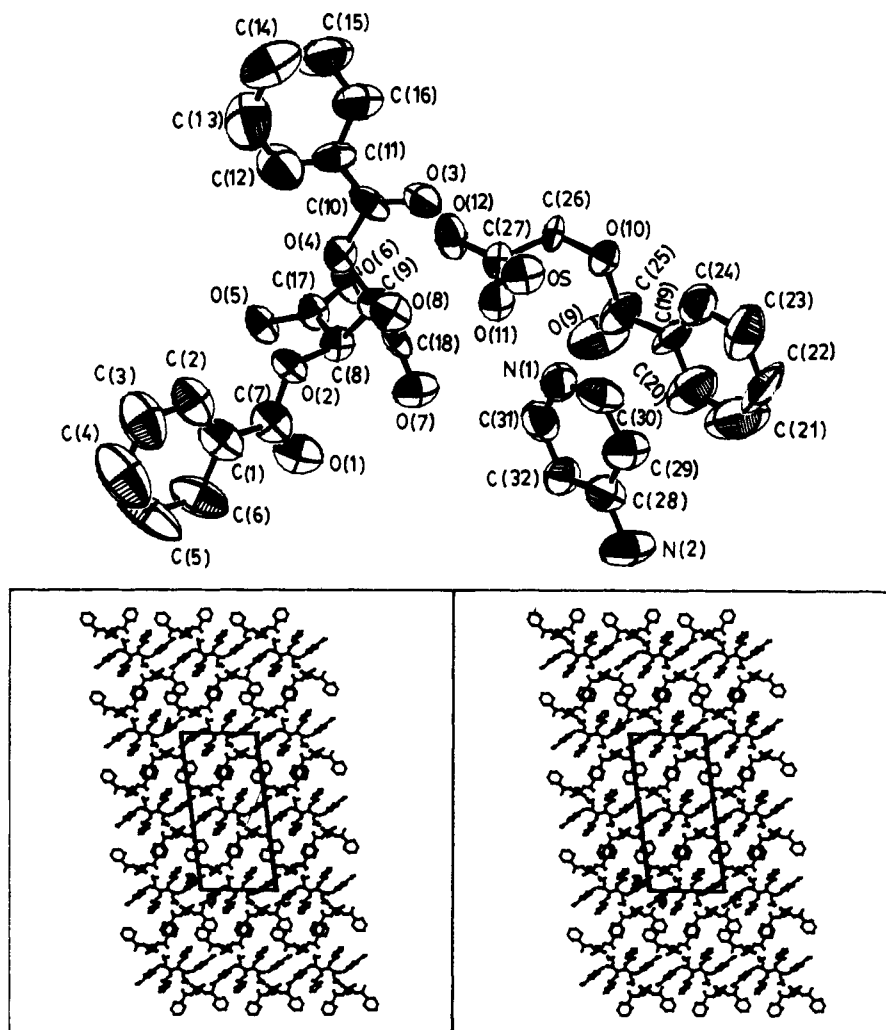


**Figure 1.** (a, top) Molecular structure of the asymmetric unit of salt III with the atom numbering scheme. (b, bottom) Stereoview of the molecular packing of salt III (viewed down the shortest axis).

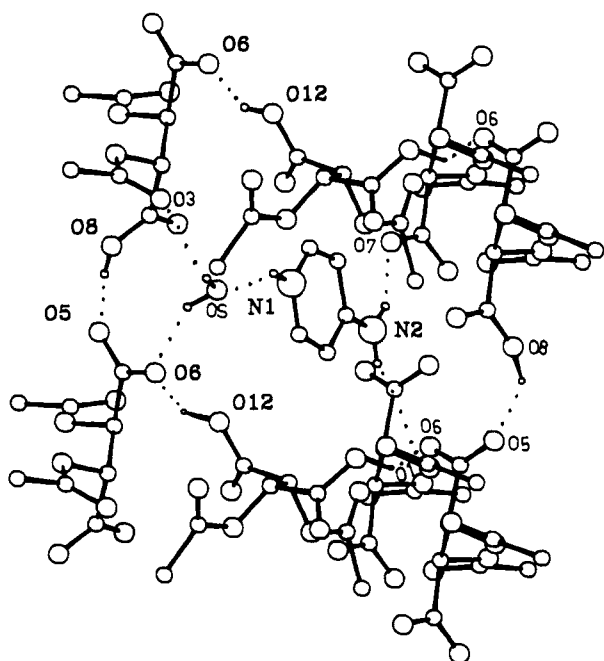


**Figure 2.** Overall hydrogen-bonding patterns in salt III (phenyl rings are not shown for the sake of clarity).

to each other.<sup>29</sup> This feature is preserved in both salts III and IV. The crystal structure of III has two types of DBT

**Table 9. Geometry of Hydrogen Bonds in Salt III\***

D-H...A	$r(\text{H}\cdots\text{A})/\text{\AA}$	$r(\text{D}\cdots\text{A})/\text{\AA}$	DH...A/deg
N(1)-H(N1)...O(S)	1.935	2.771	146.8
O(S)-H(OS1)...O(3)	2.349	2.982	125.0
O(12)-H(O12)...O(6)	1.852	2.531	141.3
O(S)-H(OS2)...O(6) <sup>1</sup>	2.113	2.896	145.9
O(8)-H(O8)...O(5) <sup>1</sup>	1.630	2.510	166.4
N(2) <sup>2</sup> -H(N21)...O(7)	2.019	2.865	161.8
N(2) <sup>3</sup> -H(N22)...O(1)	2.082	2.945	163.0

\* Symmetry elements: <sup>1</sup>X, 1 + Y, Z; <sup>2</sup>-X, Y, -Z; <sup>3</sup>-X, Y - 1, -Z.

moieties. One is in the monoanionic (COO<sup>-</sup>-COOH) form and the other is in the diacid form. The 4-AP moiety remains protonated (4-APH<sup>+</sup>) via ring nitrogen. This is clear from the consideration of bond distances and angles of the reported X-ray structure of free 4-AP (II) and its protonated analogues (Table 7). In the crystal structure of free 4-AP,<sup>30</sup> the bond distance of exocyclic nitrogen to the ring carbon is found to be 1.363(3) Å. This value is considerably reduced in 4-aminopyridinium hemiperchlorate<sup>31</sup> [1.343(4) Å] and also in 4-AP moiety in III [C(28)-N(2) = 1.319(13) Å]. This suggests that the

(29) Parafonry, A.; Tinant, B.; Declercq, J. P.; Van Meerssche, M. *Bull. Soc. Chim. Belg.* **1983**, *92*, 437.

(30) Chao, M.; Schempp, E. *Acta Crystallogr., Sect. B, Struct. Sci.* **1977**, *33*, 1557.

(31) Teulon, P.; Delaplane, R. G.; Olovsson, I.; Roziere, J. *Acta Crystallogr. Sect. C, Cryst. Struct. Commun.* **1985**, *41*, 479.

Table 10. Geometry of Hydrogen Bonds in Salt IV<sup>a</sup>

D-H...A	$r(\text{H}\cdots\text{A})/\text{\AA}$	$r(\text{D}\cdots\text{A})/\text{\AA}$	DH...A/deg
N(1)-H(N1)...O(1)	1.933	2.822	150.8
O(7)-H(O7)...O(5) <sup>1</sup>	1.447	2.470	171.4
N(2)-H(N22)...O(6) <sup>2</sup>	1.856	2.806	162.2
N(2)-H(N21)...O(8) <sup>3</sup>	1.941	2.866	161.0

<sup>a</sup> Symmetry elements: <sup>1</sup>1 + X, Y, Z; <sup>2</sup>1 + X, Y, 1 + Z; <sup>3</sup>1 - X, 0.5 + Y, 1 - Z.

delocalization of the unshared pair of electrons on exocyclic nitrogen is more pronounced in protonated 4-AP than that in nonprotonated one. A systematic analysis<sup>32</sup> also suggests that an extraannular hydrogen is attached to the heterocyclic nitrogen N(1) of the 4-AP moiety in III.

However, in III the dibenzoyltartaric acid (DBT) moiety is in two distinct conformations (Table 8). Interestingly, the crystallographic 2-fold axis passes through the DBT molecules that are in the *diacid* form (DBT-C2), and the COO-COOH form is in a general position (DBT-G). The 4-AP abstracts a proton (through the pyridine N) from one of the COOH group in DBT-G to render the former monoanionic. The 4-NH<sub>2</sub> substituent of 4-AP is linked to two symmetry-related DBT-G molecules via hydrogen

bonding with the COOH of one of the DBT-G molecules (N2...O7 = 2.865 Å) and with the -OCOPh (benzoylcarbonyl oxygen) of the other DBT-G (N2...O1 = 2.945 Å). In this salt, a water molecule acts as a bridge by accepting the H from 4-APH<sup>+</sup> (OS...N1 = 2.771 Å) and by donating its two H's to COO<sup>-</sup> anion (OS...O6 = 2.896 Å) and -OCOPh (OS...O3 = 2.982 Å) of two symmetry-related DBT-G molecules. It may be noted that the DBT-G molecules are in association with each other through COO-COOH hydrogen bonds (O8...O5 = 2.510 Å), and such connectivity is extended along crystallographic *b* axis. In the intervening spaces within two such parallel, extended chains reside DBT-C2 molecules through hydrogen bonding between COO<sup>-</sup> from DBT-G and COOH of DBT-C2 (O12...O6 = 2.531 Å) on either side of the 2-fold axis (Figure 2, Table 9). Besides extensive hydrogen bonding, significant aromatic-aromatic stacking interactions are also observed. These interactions could bring further stability in the crystal packing. The most significant interaction of this kind is the one between aminopyridine ring and the benzene ring of DBT-C2 where the centroid-to-centroid distance is found to be 3.83 Å and the angle between them is 7.07°.

**Crystal Structure of IV.** An ORTEPII<sup>28</sup> view of the asymmetric unit with atom numbering scheme and the

(32) Singh, C. *Acta Crystallogr.* 1965, 19, 861.

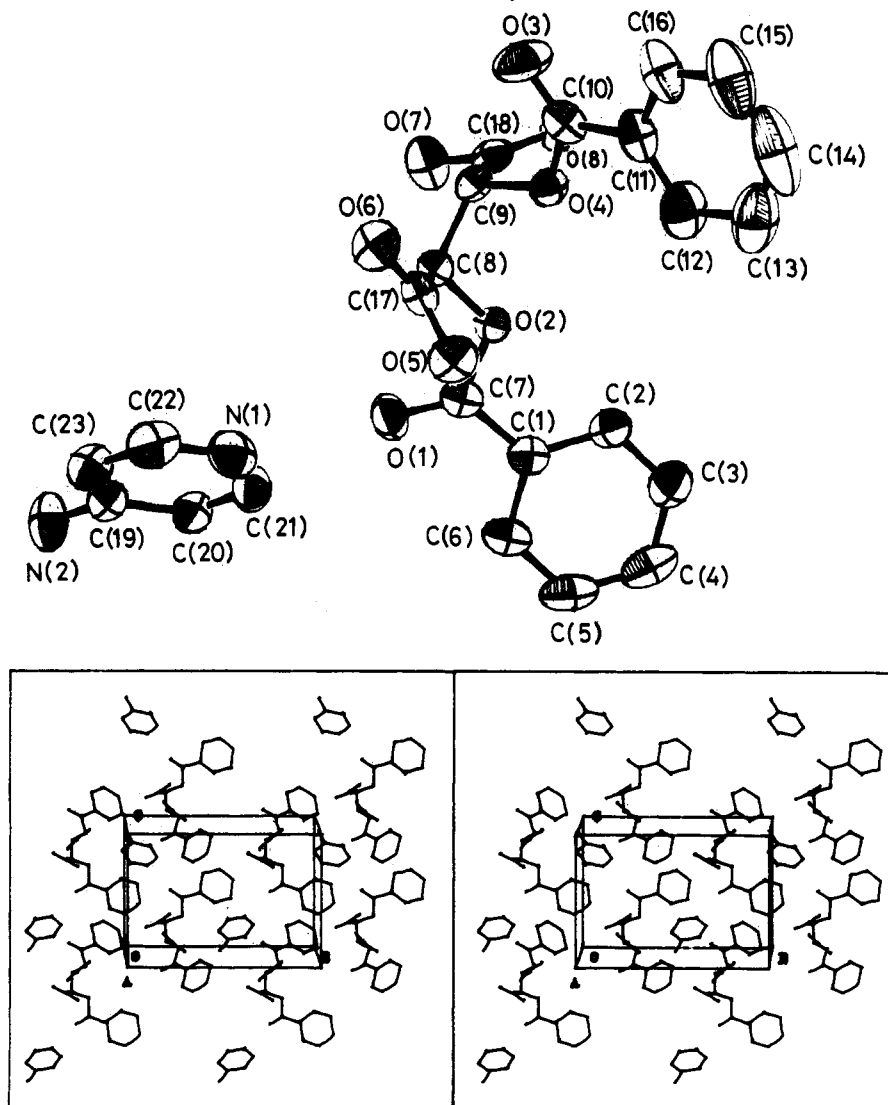
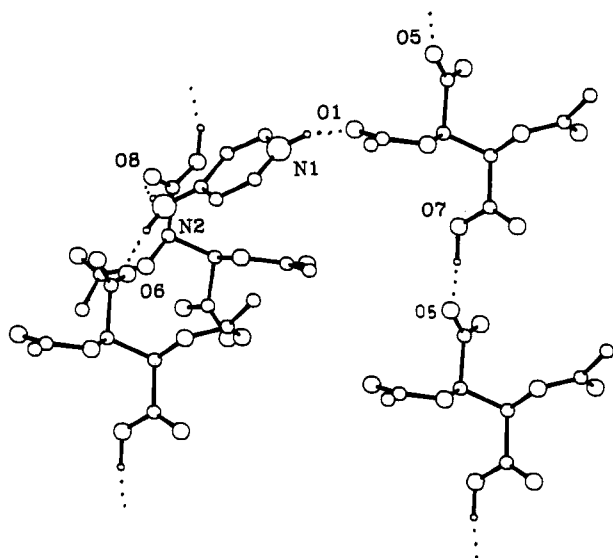


Figure 3. (a, top) Molecular structure of the asymmetric unit of salt IV with the atom numbering scheme. (b, bottom) Stereoview of the molecular packing of salt IV (viewed down the shortest axis).



**Figure 4.** Overall hydrogen-bonding patterns in salt IV (phenyl rings are not shown for the sake of clarity).

stereo packing diagram of the salt IV is shown in the Figure 3. The salt IV is not hydrated as the difference map does not indicate any water molecule in the crystal lattice. Here again, the DBT moiety is in monoanionic form and the 4-AP is protonated via its ring nitrogen (same argument as in III, Table 7). However, the DBT moiety in IV is frozen into a conformation similar to DBT-G in III (Table 8). Similar concatenating hydrogen bonded DBT network as in III persists in IV also. Thus, the 4-APH<sup>+</sup> ion makes hydrogen bonded contact with -OCOPh of DBT (N1...O1 = 2.822 Å) and the 4-NH<sub>2</sub> group holds two symmetry-related DBT molecules through hydrogen bonding via COO<sup>-</sup> (N2...O6 = 2.806 Å) and COOH functions (N2...O8 = 2.866 Å; Figure 4, Table 10).

Examination of hydrogen bonding network based on Etter's<sup>33</sup> analyses, allows us to assign the first-order network of these salts as  $N_1 = C_1^1(7)C_1^2(9)$  5D for salt III and  $N_1 = C_1^1(7)$  3D for salt IV. This represents the hydrogen-bonding patterns in these salts in a simple way. Both the salts have infinite chain of repeat unit seven  $\{C_1^1(7)\}$  which is generated as a result of head-to-tail link between adjacent DBT anions. Structure III has another nine-membered chain  $\{C_1^2(9)\}$  which is resulted from the cross-linking between adjacent infinite anionic chains of DBT and neutral DBT-C2 molecules. Salt III has five dimeric (D) hydrogen bonds, three of them are of N-H...O type and the rest are of O-H...O type. On the other hand, salt IV has three dimeric hydrogen-bonding interactions and all of them are of N-H...O type.

The crystal structures of III and IV show that there are three distinctly different conformations of DBT that are present (Table 8). All three conformations of DBT adopt the generally found conformation in diacyltartaric acid derivatives.<sup>29</sup> But the relative orientations of the phenyl rings are significantly different in each conformation. Thus, the angle between the least-squares (L.S.) planes passing

through the phenyl rings are 15.3° in DBT-G, 31.8° in DBT-C2, and 46.2° in DBT in IV. While it is important to recognize that often crystals obtained may not be of the lowest energy form even if they are the only form that can be isolated,<sup>34</sup> extensive hydrogen bonding and significant aromatic-aromatic interactions might compensate for the energy-expensive conformations of DBT species within the crystal. Optimization of various inter- and intramolecular forces in the salts III and IV, must play a significant role in reorganizing such conformations.

Finally, powder measurement showed that both salts were SHG active and their SHG intensities were 1.4–1.6 times that of urea. DBT (I) itself showed significant SHG activity but its lower mp (90 °C) and hygroscopic nature makes it less attractive for application purpose.

## Conclusions

The hydrogen-bonding-directed cocrystallization of I and II has been extensively studied in this work. The key element in this design strategy employs a chiral dibenzoyltartaric acid derivative. This molecular component ensures crystallization into a noncentrosymmetric space group, an important requirement for nonlinear optical activity. The preparative procedures are simple and general. The solids are colorless and optically transparent have favorable solubility properties and fairly high melting points. As a consequence, these are useful materials with good mechanical properties and thermal stabilities for doping. Additionally, the flexibility in achieving salts with different stoichiometries could be helpful in getting different packing modes which is an important aspect of crystal engineering. We recognize, however, that the presence of a noncentrosymmetric space group does not ensure the maximum nonlinear effect. It is further necessary that the molecular components have the proper orientation with respect to each other for an optimal NLO response. Nevertheless, this strategy of using chiral anions to orient the aminopyridinium ion may be useful for designing novel NLO materials. The directional character as well as the strength of the hydrogen bond, in conjunction with the specific hydrogen bonding and stacking interaction characteristics displayed by dibenzoyl D-tartrate ions generates a tool that may be utilized for further designing of molecular materials.

**Acknowledgment.** We thank Professor C. N. R. Rao and Department of Science and Technology, New Delhi, India, for financial support, Prof. K. Venkatesan for useful discussions, Prof. C. K. Subramanian, Mr. B. R. Prasad, and Ms. Renuka K. for SHG measurements. P.D. thanks University Grants Commission, India, for a senior research fellowship. We thank the two referees for their valuable comments.

**Supplementary Material Available:** Tables of fractional atomic coordinates and equivalent isotropic thermal parameters of the title compound (17 pages); tables of observed and calculated structure factors (8 pages). Ordering information is given on any current masthead page.

(33) Etter, M. C.; MacDonald, J. C. *Acta Crystallogr., Sect. B, Struct. Sci.* 1990, 46, 256.

(34) Etter, M. C. *J. Phys. Chem.* 1991, 95, 4601.